The Stochastic Time Delay Model and Prediction for Space Teleoperation

Tianjian Hu[1] and Xuexiang Huang.[2]
Beijing Institute of Tracking and Telecommunication Technology, Beijing, China, 100094

Qian Tan[3]
Beijing Institute of Tracking and Telecommunication Technology, Beijing, 100094, China

Space teleoperation means an extension of human operator's intelligence to the remote telerobot in the space, and has been widely applied in space exploration and service. The main difficulty in teleoperation is the large stochastic time delay between operator and telerobot. Previous works on space teleoperation mainly focus on the control design, and some researches also give good solutions to the prediction of net work time delay, but few has been put forward to give a sufficient analysis and precise prediction for time delay in space situation. This paper conducts a study upon the time delay measure, model and prediction for space teleoperation. Time delays produced by different nodes of the space-ground round trip are measured and analyzed using statistical methods. And probability density distribution models are proposed and verified by parameter Maximum Likelihood Estimation (MLE) and χ^2 Goodness of Fit Principle Test (GFT). Steps above show that in our teleoperation system, uplink time delay is a short-term autocorrelated sequence varying between 1.05s and 1.20s. Then, based on Non-Gaussian Auto-Regressive Model (NGAR) and Kalman Filtering (KF), uplink time delay sequence is predicted with absolute error less than 80ms and relative error below 8%. Finally, computer simulation results show that motion precision simulated by the virtual model of the telerobot will be improved with predicted value of the uplink time delay compensated, and future work is outlined in the end of this paper.

I. Introduction

SPACE teleoperation is a significant way for space operation including On-orbit Servicing[1,2], In-space Experiment[3,4], and Planet Surface Exploration[5]. It is well-known that the large statistical time delay (TD) existing in the space-ground round trip performs a side effect to the stability and tracking ability of the space telerobot. Without the knowledge of the TD, no appropriate controller especially its parameters could be obtained. And the interest on the work related to the TD has never faded out. In the early study focusing on the control scheme design and algorithm, though the randomicity has already been aware of, TD is treated simply as a constant value[6]. As researches progress, the characteristics of TD have attracted more and more attention. In 7 and 8, round trip TD over network is measured and analyzed using time series, histogram and phase plot under two different communication circumstances. Basic characteristics of TD series over network have been realized, and due to the large amount of factors influencing the value, it seems impossible to establish an analytical model for TD and the prediction turns to be a difficult job. So in the later literatures, researchers keep their eyes on prediction based on statistic theory and develop series of methods such as Auto-Regressive Model[9, 10], Maximum Entropy Principle[11], and Sparse Multivariate Linear Regressive Models[12]. With these tools presented above, precise prediction results have been achieved towards teleoperation over the Internet.

Although network is commonly used, huge differences exist between TD over network and the one in space situation. In space teleoperation system, the transmission route of the signal over network is more determinate, and the bandwidth is assured. Second, a kind of real-time protocol such as UDP protocol is applied, instead of the

[1] Assistant Professor, Beijing Institute of Tracking and Telecommunication Technology (BITTT), 26# Beiqing Rd. Haidian District Beijing China.
[2] Associate Professor, BITTT, 26# Beiqing Rd. Haidian District Beijing China.
[3] Associate Professor, BITTT, 26# Beiqing Rd. Haidian District Beijing China.

traditional TCP/IP protocol. Third, the load of the connection is relatively stable during the period of teleoperation. And lastly there are many unique nodes including wireless signal transmission and operation center, ground station and satellite computation existing in the round trip.

As few works have been proposed, this paper devotes itself to a detailed study on the stochastic TD model and prediction for space teleoperation. In addition, the improvement for a virtual telerobot model with predicted TD series compensated is shown by computer simulations. The rest of this paper is structured as follows. In the next section, the source for the space-ground round trip TD is analyzed and in order to measure the various kinds of TDs, some test systems are established intentionally. In section three, based on results of the measurement, statistical characteristics including histogram, phase plot and autocorrelation are presented, and probability density functions for different kinds of TDs are established by Maximum Likelihood Estimation (MLE) and χ^2 Goodness of Fit Principle Test (GFT). As uplink TD series is short-term autocorrelated and distributes to a non-Gaussian distribution, section four considers conducting a prediction based on Non-Gaussian Auto-Regressive Model (NGAR) and Kalman Filtering (KF). With predicted TD series compensated, some computer simulations are conducted for a planar series link model with 3 degree-of-freedom (DOF) in an agravic environment in section five. Finally, in section six conclusions of this paper are drawn and future works are outlined.

II. Measurements for Time Delay Series

This section mainly discusses two problems including where TDs come from and how to acquire their detailed values. For the first question, this section analyzes sources for space-ground round trip TD, and concludes that TDs generally come from wireless signal transmission, data transmission over network and data processing. For the second one, measure systems are established particularly for statistical kinds of TDs and measure results are obtained.

A. Sources for Space-Ground Round Trip Time Delay

With large amounts of equipments in it, detailed structure of space teleoperation system is quite complicated. However, if some nodes are considered as black boxes, a relatively simple scheme for space teleoperation system can be shown as Figure 1. Generally speaking, TD comes from wireless communication, network, and data processing nodes including telerobot, ground station, and operation center.

Denote uplink and downlink TD as τ_U and τ_D. Define the uplink TD τ_U as the time interval between operation center sends up commands and telerobot receives commands and starts working, and the downlink τ_D as the time interval between telerobot begins to sample its own motion states and operation center generates control commands. So three formulas are obtained as follows

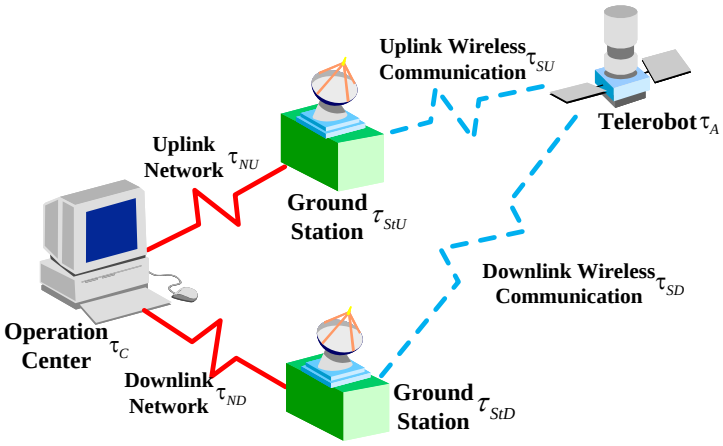

Figure 1. Basic scheme for space teleoperation system.

$$\tau_U = \tau_A + \tau_{NU} + \tau_{StU} + \tau_{SU} \tag{1}$$

$$\tau_D = \tau_C + \tau_{ND} + \tau_{StD} + \tau_{SD} \tag{2}$$

$$\tau = \tau_U + \tau_D \tag{3}$$

Since TD due to wireless communication can be derived from the physical range between ground station and telerobot and present radio exterior measuring equipments can provide an accurate rage measure result, prediction error of TD over wireless communication can be restrained under 10^{-5}ms for low-earth-orbit (LEO) telerobots. Thus, this paper does not care too much about this part of TD and just keep an eye on the statistical TD.

B. Measure System and Result for Round Trip Time Delay over Network

The test for round trip time delay over network (RTTN) was taken between Beijing and Xi'an (approximate 900km far away). A stream of data packets at local site, Beijing Institute of Telecommunication and Tracking Technology, based on UDP protocol with packet rate equaling $\delta = 1s$ and 64 bytes per packet as the length was transmitted to the remote site, Xi'an Satellite TT&C Center some day. The bandwidth of the network was chosen as 2M. The RTTN series with duration of 300s is shown in Figure 2. Here the clock of windows operation system was used as the time baseline and the time excursion of this clock in 1 second will not exceed 0.1ms, so the precision of measurement can be assured.

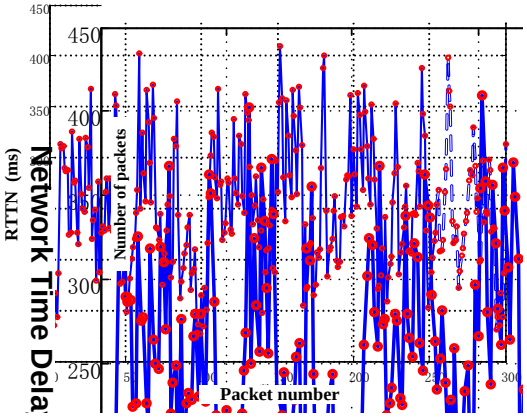

Figure 2. Plot of RTTN series.

Obviously, RTTN series is a random variable between 125ms and 425ms. Different from teleoperation over network, network used here is designed particularly with packet loss rate below 10^{-3} and relatively much more stable work load. So the statistical characteristics vary little in different measure periods, and a further analysis dependent on plot in figure 2 will offer a credible result.

C. Measure System and Result for Uplink Data Processing Time Delay

Operation center, ground station and telerobot are the special data processing nodes for space teleoperation and in order to measure the uplink data processing time delay (UDPTD), these nodes were integrated into a measure system， shown as figure 3.

In figure 3, operation center, ground station and telerobot were connected with each other by fiber on the local site. Data packet with $\delta = 1s$ as packet rate and 64 bytes as packet length was sent by operation center to telerobot through fibers and ground station. Since fibers in the system are shorter than 100m, TD generating from fiber transmission could be easily ignored. Further more, the measure system was designed as an open-loop system, so GPS timing equipment was introduced to provide a clock with time excursion below 100ns. The test lasted 3500s and figure 4 shows the plot of UDPTD series. Unlike RTTN series, UDPTD series shown in figure 4 is much more stable. In a short-term period lasting 8s, the dithering of UDPTD series is less than 10^{-3}ms, then the series jumps to another stable short-term period. The total dithering won't exceed 3.5ms, which is only 2.3% of the dithering of the uplink RTTN suppose that uplink TD equals downlink TD.

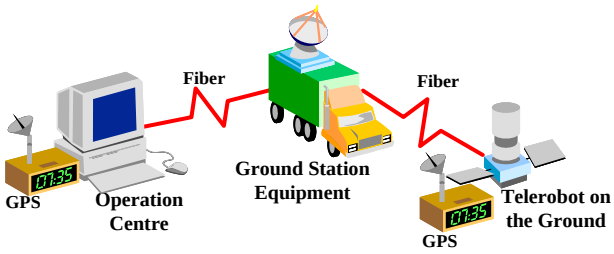

Figure 3. Measure system for UDPTD.

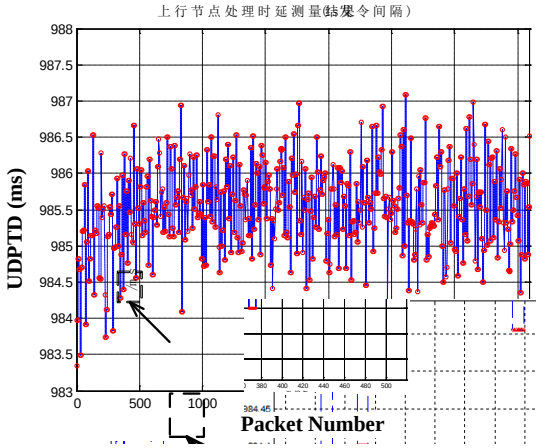

Figure 4. Plot of UDPTD series.

Above all, measurements conducted in this section offer some basic knowledge about the TD, which is a statistical series with value between 2.10s and 2.40s, for space teleoperation, and a further study on statistical characteristics could be given based on it.

III. Statistical Characteristics of Time Delay

The following section works on the statistical characteristics of RTTN and UDPTD based on measure results, which can also be called sampling in Statistics. Similarly to literature 7 and 12, as the beginning part of this section histogram, phase plot and autocorrelation are applied here to find more information: histogram has a closed connection with the probability density distribution of a random variable; phase plot shows the one-step

autocorrelation of TD and can reflect the working load of the entire system in some sense; and autocorrelation shows the relationship between the present value of a random variable and its past values. In the second part of this section, assumptions of the probability density function are made based on the knowledge of histogram of the RTTN and UDPTD sampling. MLE and χ^2 GFT methods are then used to derive and verify detailed forms of functions.

A. Histogram, phase plot and autocorrelation

Figure 5 and 6 give the histograms for RTTN sampling with 25ms as the time interval and UDPTD sampling with 0.25ms as the time interval. And probability density of UDPTD may distribute to a Gaussian distribution, while RTTN seems to distribute to a non-Gaussian distribution.

Figure 7 and 8 present the phase plot for RTTN and UDPTD. Plots on both of these two figures cluster around the line $t(i+1) = t(i)$, which indicates that both network communication and data processing are non-congested. On the other hand, there are still some differences between figure 7 and figure 8. In figure 7, plots cluster dispersedly around the line $t(i+1) = t(i)$ because RTTN is entirely stochastic, while in figure 8 plots centralize around the line due to the short-term stabilization of UDPTD.

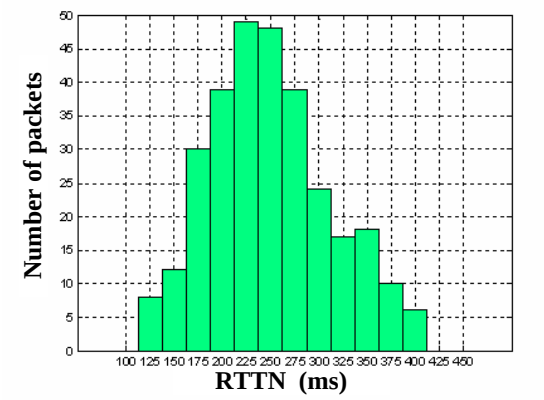

Figure 5. Histogram of RTTN.

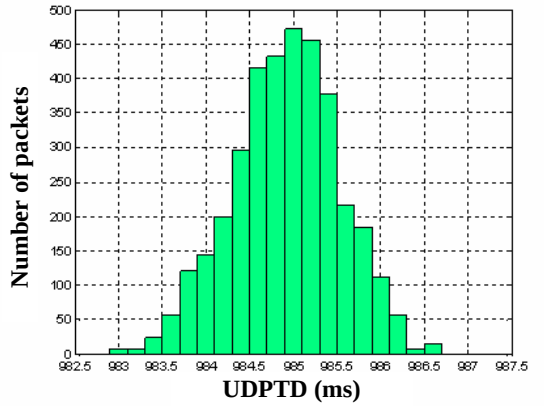

Figure 6. Histogram of UDPTD.

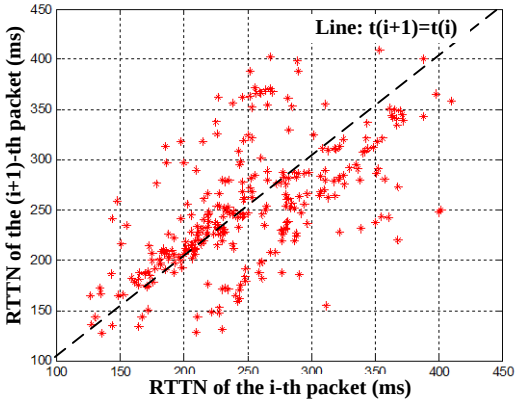

Figure 7. Phase plot of RTTN.

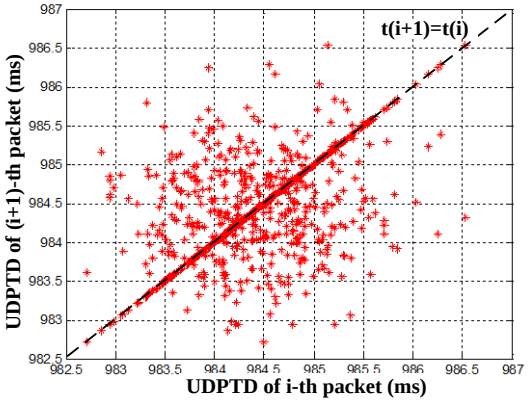

Figure 8. Phase plot of UDPTD.

Autocorrelation is computed as follows

$$C(\Delta) = \frac{\sum_{i=1}^{N-\Delta} (x_i - \overline{x})(x_{i+\Delta} - \overline{x})}{\sum_{i=1}^{N} (x_i - \overline{x})^2} \tag{4}$$

where $\{x_i\}$ is the random series, N is the length of the series, $\overline{x}$ is the average of $\{x_i\}$, and Δ is the number of step. With the definition shown as Eq. (4), a sharp peak can be seen in both figure 9 and figure 10, which indicates the randomness of RTTN and UDPTD. However, a short-term autocorrelation can also be seen after enlarging the peak of the figure: for RTTN, autocorrelation holds above 0.2 in 3 steps and for UDPTD this value does not decrease to

0.1 after 8 steps. Thus, prediction method such as auto-regressive model is hoped to be used based on this special characteristic.

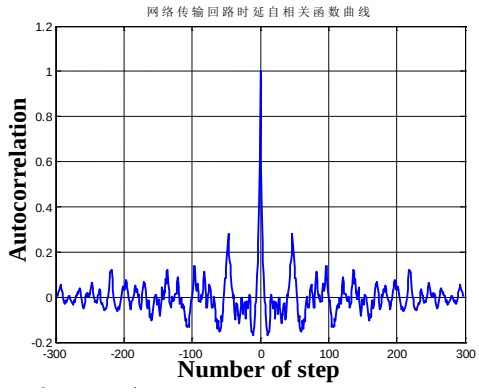

Figure 9. Autocorrelation of RTTN.

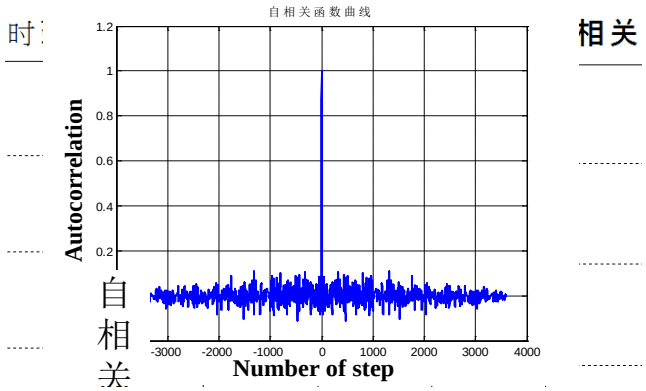

Figure 10. Autocorrelation of UDPTD.

B. Probability density function

According to the observation of histogram shown as figure 5 and 6, the probability density distribution of RTTN is assumed to take a Gamma form and the one of UDPTD is assumed to take a Gaussian form, which are shown as follows

Gamma Distribution for RTTN
$$f(x|\lambda,r)=\begin{cases}\dfrac{\lambda^{-r}}{(r-1)!}x^{r-1}\exp(-x/\lambda), & x>0\\ 0, & x\le 0\end{cases} \tag{5}$$

Gauss Distribution for UDPTD
$$f(x\,|\,\mu,\sigma)=\frac{1}{\sqrt{2\pi}\sigma}\exp\left[-\frac{(x-\mu)^2}{2\sigma^2}\right] \tag{6}$$

where parameters including λ, r, μ and σ need to be estimated. In Statistics, it is natural to make these assumptions from the histogram, but they remain to be tested and verified. MLE and χ^2 GFT methods are commonly used in such a case, and a brief introduction to these methods is given in the following content.

Suppose the probability density distribution function of a random variable x is given as $f(x|t)$, in which t is the estimated parameter vector. Then the maximum likelihood function can be derived as

$$L(t)=\prod_{i=1}^{n} f(x_i\,|\,t) \tag{7}$$

or the logarithm form of the function is given as

$$\ln L(t)=\sum_{i=1}^{n}\ln f(x_i\,|\,t) \tag{8}$$

where x_i is the sampling. The MLE value of parameter vector t is attained when maximum likelihood function reaches its extremum, i.e.

$$\partial \ln L(t)/\partial t=0 \tag{9}$$

With Eq. (9) solved, the estimation of parameters can be attained. However, formulas above do not guarantee the validity for the assumption, so the verification needs to be taken after the assumption and MLE steps. Here, a kind of method named χ^2 Goodness Fit Test is adopted with statistical variableχ^2 constructed as follows

$$\chi^2 \triangleq \sum_{i=1}^{m} \frac{(n_i - np_i)^2}{np_i} \tag{10}$$

where the interval $[0,+\infty)$ is divided into m sub-intervals as $[0,a_1)$, $[a_1,a_2)$,$\cdots$ $[a_{m-1}, +\infty)$, n is the total amount of the sampling, n_i is the amount of sampling in the sub-interval $[a_i,a_{i+1})$, and p_i is the probability of the random variable x appearing in the same sub-interval. The probability density distribution of variable constructed as formula (10) is named as χ^2 Distribution, and assumptions shown as Eqs. (5) and (6) satisfy the measure sampling with distinguish level equal to α if the following Inequation is obtained

$$\sum_{i=1}^{m} \frac{(n_i - np_i)^2}{np_i} \le \chi^2_{1-\alpha}(m-k-1) \tag{11}$$

where k is the dimension of the vector t, and $\chi^2(m\text{-}k\text{-}1)$ can be looked up from the table in Statistic handbooks.

With methods presented above, parameters are estimated as $\lambda = 2.688$, $r = 25$, $\mu = 984.92ms$ and $\sigma = 0.61ms$ when distinguish level α equals 0.005 for both RTTN and UDPTD sampling. Generated by Eqs. (5) and (6), figure 11 and figure 12 give another two histograms whose basic distribution features are similar to figure 5 and figure 6.

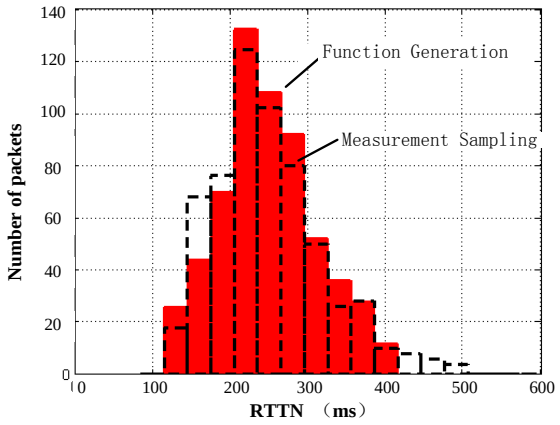

Figure 11. Histogram of Gamma distribution.

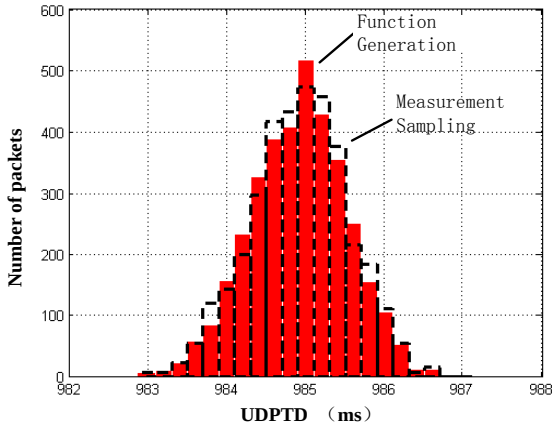

Figure 12. Histogram of Gauss distribution.

IV. Uplink Time Delay Prediction

Autocorrelation values shown as figure 9 and 10 indicate that TD obtains a short-term autocorrelated characteristic, so an Auto-Regressive (AR) model is hoped to give a precise prediction for the future value of TD series. However, the Gamma distribution of RTTN doesn't satisfy the Gauss distribution precondition of AR theory, which leads to an obstacle to use the classical AR model directly. Fortunately, this kind of problem has been successfully solved by literatures 13-14 using higherorder statistics. And in this section, the cumulant is applied as a kind of higherorder statistics directly to establish an NGAR model for uplink time delay (UTD) and make the prediction based on KF. Since prediction error of TD over wireless communication can be easily restrained under 10^{-5}ms, prediction here is mainly conducted towards statistical parts of UTD including uplink time delay over network (UTDN) and UDPTD.

A. Non-Gaussian Auto-Regressive Model for Uplink Time Delay

In practical measurement, UTDN (half of RTTN) and UDPTD are mixed together and it is impossible to separate them from each other. If $\{y_t\}$ denotes the measured series of UTD, $\{x_t\}$ denotes the series of UTDN, and $\{v_t\}$ denotes the series of UDPTD, the observation of TD can be treated as the summation of the state variable x_t and a white noise v_t.

Fist the state equation for UTDN is established based on NGAR theory, the basic form is as follows

$$x_t = \sum_{i=1}^{n} \varphi_i x_{t-i} + a_t \tag{12}$$

in which n denotes the order of the NGAR, $\varphi = [\varphi_1 \quad \varphi_2 \quad \cdots \quad \varphi_n]^T$ denotes the auto-regressive coefficient, and a_t denotes the additional process white noise. Then the cumulant of $\{x_t\}$ is used to identify n and φ. The definition is given as

$$c_k = cum\left(x_1, x_2, \cdots, x_k\right) = \left(-j\right)^k \left. \frac{\partial^k \ln \Phi(\omega_1, \omega_2, \cdots \omega_k)}{\partial\omega_1 \partial\omega_2 \cdots \partial\omega_k} \right|_{\omega_1=\omega_2=\cdots=\omega_k=0} \tag{13}$$

where function Φ is defined as

$$\Phi(\omega_1, \omega_2, \cdots \omega_k) \overset{def}{=} E\left\{\exp\left[\, j\left(\omega_1 x_1 + \omega_2 x_2 + \cdots + \omega_k x_k\right)\right]\right\} \tag{14}$$

The main benefit from cumulant is that for any order higher than 3 the cumulant equals zero for Gauss series, so a kind of modified Yule-Walker equation can be obtained as

$$c_{ky}\left(\tau_1, \tau_2, 0, \cdots, 0\right) = \sum_{j=1}^{n} \varphi_j c_{ky}\left(\tau_1 - j, \tau_2, 0, \cdots, 0\right), \quad \tau_1 > 0 \tag{15}$$

In Eq. (15) k is chosen as 3, and the determine matrix $\bar{C}$ is formalized to get the order n of NGAR.

$$\bar{C} = \begin{bmatrix} c_{ky}\left(1, -\bar{n}\right) & \cdots & c_{ky}\left(\bar{n}, -\bar{n}\right) \\ \vdots & \vdots & \vdots \\ c_{ky}\left(1, 0\right) & \cdots & c_{ky}\left(\bar{n}, 0\right) \\ c_{ky}\left(\bar{n}, -\bar{n}\right) & \cdots & c_{ky}\left(2\bar{n}-1, -\bar{n}\right) \\ \vdots & \vdots & \vdots \\ c_{ky}\left(\bar{n}, 0\right) & \cdots & c_{ky}\left(2\bar{n}-1, 0\right) \end{bmatrix} \tag{16}$$

where $\bar{n}$ is the upper limitation of the series length. Then n equals the maximum difference between neighbored singularities.

Similarly take k=3, $\tau_1 = 1, 2, \cdots, n$ and $\tau_2 = l$ in Eq. (15), then a linear equation about parameter φ is as follows

$$C\varphi = c \tag{17}$$

where

$$C = \begin{bmatrix} C\left(-n\right) \\ C\left(-n+1\right) \\ \vdots \\ C\left(0\right) \end{bmatrix}_{n(n+1)\times n} \qquad c = \begin{bmatrix} c\left(-n\right) \\ c\left(-n+1\right) \\ \vdots \\ c\left(0\right) \end{bmatrix}_{n(n+1)\times n} \tag{18}$$

and

$$C(l)=\begin{bmatrix} c_{3y}(0,l) & c_{3y}(-1,l) & \cdots & c_{3y}(1-n,l) \\ c_{3y}(1,l) & c_{3y}(0,l) & \cdots & c_{3y}(2-n,l) \\ \vdots & \vdots & \vdots & \vdots \\ c_{3y}(n-1,l) & c_{3y}(n-2,l) & \cdots & c_{3y}(0,l) \end{bmatrix} \tag{19}$$

$$c(l)=\left[c_{3y}(1,l),c_{3y}(2,l),\cdots,c_{3y}(n,l)\right]^T$$

The auto-regressive coefficient can be calculated by the least squares estimation then. Finally the estimation of a_t is given as

$$\hat{\sigma}_a^2=\frac{1}{N-n}\sum_{t=n+1}^{N}\left(x_t-\sum_{i=1}^{n}\varphi_i x_{t-i}\right)^2 \tag{20}$$

so that every parameter in Eq. (12) is determined and the state equation is obtained.

B. Kalman Filtering and Prediction Results

The UTD prediction is conducted based on the state space of the linear discrete system

$$\begin{aligned} X(t)&=\Phi(t,t-1)\cdot X(t-1)+\Gamma(t,t-1)\cdot w(t-1) \\ y(t)&=h(t)\cdot X(t\text{-RTTD}')+v(t\text{-RTTD}') \end{aligned} \tag{21}$$

where $X(t)=[x_t,x_{t\text{-}1},\cdots,x_{t\text{-}(n\text{-}1)}]^T$, $\Gamma(t,t-1)=I_n$, $Q_w=\sigma_a^2 I_n$, $w(t\text{-}1)=[a_t,a_{t\text{-}1},\cdots,a_{t\text{-}(n\text{-}1)}]^T$, $h(t)=[1\ 0\ \cdots\ 0]$, $y(t)=y_t$, $v(t)=v_t$, $R_v=\sigma_v^2 I_n$, state transfer matrix $\Phi(t,t-1)$

$$\Phi(t,t-1)=\begin{bmatrix} \varphi^T \\ I_{n-1} \quad 0 \end{bmatrix} \tag{22}$$

and RTTD' which is an integer related to the value of RTTD equals 3 in the situation of this paper.

Derived from the state space shown as Eq. (21), the prediction step of state vector, observation vector and variance matrix can be obtained using the classical KF method, and initials of state vector and variance matrix are given as

$$\hat{X}(t_0\,|\,t_0)=\left[y_{t_0} \quad y_{t_0-1} \quad \cdots \quad y_{t_0-(n-1)}\right]^T-\mu_v\cdot(1)_{n\times 1} \tag{23}$$

and

$$\hat{p}(t_0\,|\,t_0)=E\left[X(t_0)X^T(t_0)\right] \tag{24}$$

There is no distinguish between steps used above and ones of classical KF, but due to the TD which leads to a special form of observation equation shown in formula (21), the optimal prediction in two steps has to been applied as the approximation of the filtering of state vector, shown as follows

$$\hat{X}(t\text{-}1\,|\,t\text{-}1)\approx\hat{X}(t\text{-}1\,|\,t-3)=\Phi(t-1,t-2)\Phi(t-2,t-3)\hat{X}(t\text{-}3\,|\,t-3) \tag{25}$$

Fig. 13 concludes the process of the algorithm presented in this section, and values including NGAR order n=8, auto-regressive coefficient φ= [0.6973, 0.0786, 0.0019, 0.0619, 0.1235, -0.1120, 0.0861, 0.0625]^T and standard variance of the white noise $\hat{\sigma}_a = 33.82ms$ are calculated step by step.

Fig. 14 and Fig. 15 present the prediction result and error. With the algorithm shown in this section, precise prediction result with error less than 80ms has been achieved. Besides, the error integration doesn't exceed 300ms, and compared to the prediction without KF, algorithm developed here performs much better.

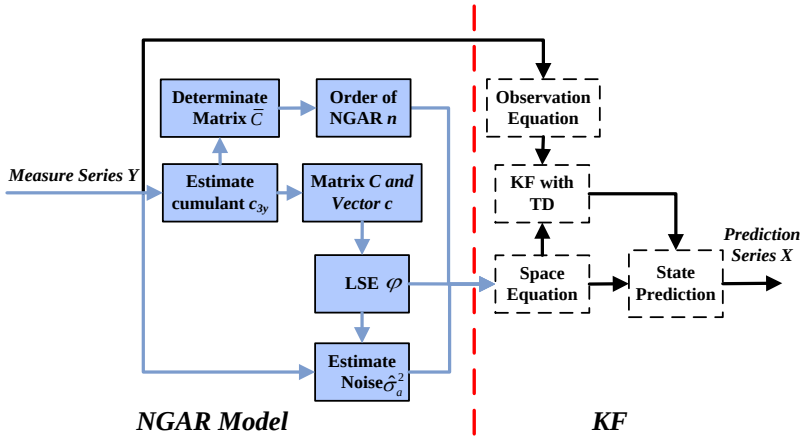

Figure 13. Process of prediction algorithm.

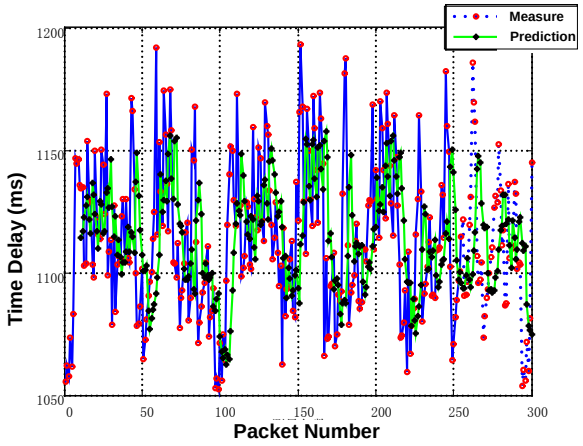

Figure 14. Prediction plot of UTD.

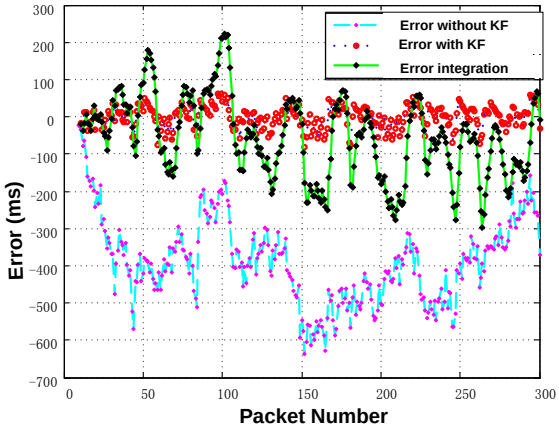

Figure 15. Prediction error of UTD.

V. Computer Simulations

UTD prediction is helpful for choosing an appropriate controller and its parameters for space teleoperation. Besides, with prediction values of UTD series compensated, virtual model of telerobot can provide a better tracking performance compared to the situation without UTD compensation, which is another important application for UTD prediction. In order to test the latter application, some computer simulation work was conducted using Matlab. First, shown in figure 16, a computer simulation system in Matlab/Simulink was established and a planar serial manipulator with 3 degree-of-freedom was chosen as the control plant. The tele-manipulator applied here is supposed to be a rigid body with mass distributed uniformly, and basic parameters of each link are given as a_1=0.985m, m_1=7.5kg; a_2=0.765m, m_2=7.0kg; and a_3=0.390m, m_3=11.9kg.

In figure 16, signal generator outputs expected joint angle as control command to telerobot through UTD measure series and to virtual model through prediction series. Both of the measured and predicted series of UTD are shown in figure 14. The telerobot and the virtual model execute received commands and the locus of telerobot's end-effector is shown in figure 17 with expected joint angle as follows

$$\theta_M = \begin{cases} \sin(\pi t/15)\cdot[\pi/2 \quad \pi/4 \quad \pi/3]^T & P_x \geq 2 \\ \sin(\pi t/30)\cdot[\pi/4 \quad \pi/8 \quad \pi/4]^T & P_x < 2 \end{cases} \tag{26}$$

where x-axis displacement of end-effector P_x is treated as the threshold for command transit.

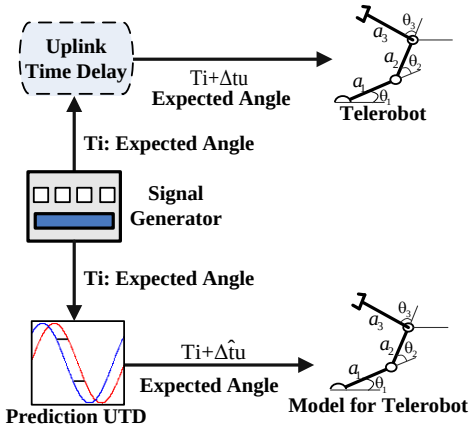

Figure 16. Computer simulation system.

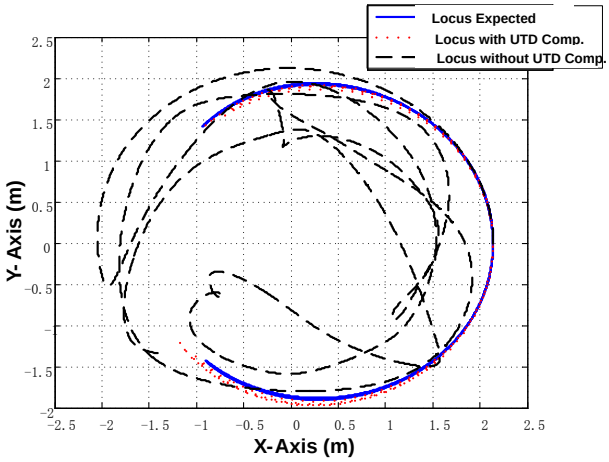

Figure 17. Locus of telerobot's end-effector.

Three kinds of loci generated by telerobot's end-effector are presented in figure 17. The real line is the expected locus, the dot line represents the locus of virtual model's end-effector with UTD prediction series compensated and the dash line represents the locus without UTD compensation. Obviously, the dot line is much more closed to the real line, which indicates a better tracking performance, especially when motion transit happens. Thus, besides a criterion for controller design, UTD prediction can also be used to improve the simulation precision of the telerobot's virtual model.

VI. Conclusions And Future Work

In this paper a detailed research on TD measurement, statistic model and prediction has been made for space teleoperation. Since there are no particular literatures on TD in space situation yet, this paper makes a contribution to the future work in space teleoperation area and draws some significant conclusions, including: 1) value of Round Trip Time Delay (RTTD) in our system is between 2.1s and 2.4s, and stochastic parts of RTTD are short-term autocorrelated; 2) algorithm based on NGAR and KF effectively predicts UTD with error less than 80ms and error integration less than 300ms; 3) performance of telerobot can be improved with UTD predicted and compensated.

In the future, more experiment data of TD is expected to accumulate and tests for the fitness of the algorithm to different communication circumstances of space teleoperation are looked forward to. What's more, the NGAR developed here needs large amounts of data training before the start of the prediction, so a recursive method for the auto-regressive coefficient estimation is hoped to be developed that real-time TD prediction can be achieved.

References

[1]Takashi Imaida, Yasuyoshi Yokokohji, Toshitsugu Doi etal., "Ground-Space Bilateral Teleoperation of ETS-VII Robot Arm by Direct Bilateral Coupling Under 7-s Time Delay Condition," *IEEE Trans. On Robotics and Automation*, Vol. 20, No. 3, 2004, pp. 499-511.

[2]R. B. Friend, "Orbital Express Program Summary and Mission Overview," *Proc. of SPIE Sensors and Systems for Space Applications II*, Vol. 6958, No. 3, 2008, pp. 1-11.

[3]G. Hirzinger, B. Brunner, J. Dietrich and etal., "Rotex-The First Remotely Controlled Robot in Space," *Proc. of IEEE Intl. Conf. on Robotics and Automation*, 8-13 May 1994, pp. 2604-2611.

[4]C. Preusche, D. Reintsema, K. Landzettel, G. Hirzinger, "Robotics Component Verification on ISS ROKVISS-Preliminary Results for Telepresence," *IEEE/RSJ Intl. Conf. on Intelligent Robots and Systems*, 2006, pp. 4595-4601.

[5]R. B. Roncoli, J. M. Ludwinski, "Mission Design Overview for the MARS Exploration Rover Mission," *AIAA/AAS Astrodynamics Specialist Conf. and Exhibit*, Monterey, California, USA., 5-8 August 2002, pp.1-24.

[6]R. J. Anderson, M. W. Spong, "Bilateral Control of Teleoperation with Time Delay," *IEEE Trans. On Automatic Control*, Vol. 34, No. 5, 1989, pp. 494-501.

[7]R. Oboe, P. Fiorini, "Issues on Internet-Based Teleoperation," *Proc. of the 5th IFAC Symposium on Robot Control*, Nantes, France, September 1997, pp. 611-617.

[8]R. Oboe, P. Fiorini, "A Design and Control Environment for Internet-Based Telerobotics," *The Intl. Journal of Robotics Research*, Vol. 17, No. 4, Apr. 1998, pp. 433-449.

[9]T. Mirfakhrai, S. Payandeh, "A Delay Prediction Approach for Teleoperation Over The Internet," *IEEE Intl. Conf. on Robotics and Automation*, Aug. 2002, pp. 2173-2183.

[10]Xiufen Ye, Liu, P.X., Guobin Li, “Statistical Analysis And Prediction of Round Trip Delay for Internet-Based Teleoperation,” *IEEE/RSJ Intl. Conf. On Intelligent Robots and Systems*, Dec. 2002, pp. 2999-3004.

[11]Liu P.X., Meng M., Xiufen Ye, Gu J, “End-To-End Delay Boundary Prediction Using Maximum Entropy Principle (MEP) for Internet-Based Teleoperation,” *IEEE Intl. Conf. On Robotics and Automation*, Aug. 2002, pp. 2701-2706.

[12]Dan Chen, Xiuhui Fu, Wei Ding and etal., “Shifted Gamma Distribution and Long-Range Prediction of Round Trip Timedelay for Internet-Based Teleoperation,” *IEEE Intl. Conf. On Robotics and Biomimetics*, Feb. 2009, pp. 1261-1266.

[13]J.M. Mendel, “Tutorial on Higher Order Statistics (Spectra) in Signal Processing and System Theory: Theoretical Results and Some Applications,” *Proceedings of the IEEE*, Vol. 79, No. 3, 1991, pp. 278-305.

[14]Swami A. and J.M. Mendel, “ARMA Parameter Estimation Using Only Output Cumulants,” *IEEE Trans. ASSP*, Vol. 38, 1990, pp. 278-305.